Desalination and Water Treatment
www.deswater.com
doi: 10.1080/19443994.2014.902333

54 (2015) 2611–2624
May

Taylor & Francis
Taylor & Francis Group

Sorption of Reactive blue 19 onto freshwater algae and seaweed

S. Devi[a,*], A. Murugappan[a], R. Rajesh Kannan[b]

[a]*Department of Civil Engineering, Annamalai University, Annamalai Nagar 608 002, Tamil Nadu, India, Tel. +91 94864 20682; email: degisvinicivil2002@yahoo.co.in*
[b]*Environmental Engineering Laboratory, Department of Chemical Engineering, Annamalai University, Annamalai Nagar 608 002, Tamil Nadu, India*

Received 21 September 2013; Accepted 27 February 2014

ABSTRACT

The potential of freshwater algae (*Spirulina platensis*) and seaweed (*Gracilaria edulis*) for removing reactive blue 19 (RB 19) were investigated using batch adsorption techniques. The effects of various experimental parameters (Solution pH, initial dye concentration, contact time, adsorbent dosage, agitation speed, particle size and temperature) have been evaluated and optimal experimental conditions were ascertained. The biomass exhibited maximum dye uptake at acidic pH (pH = 1.5) due to electrostatic interactions between the biomass and the dye particles. Several isotherm models like, Langmuir, Freundlich, Dubinin–Radushkevich and Temkin adsorption isotherms were employed to monitor the adsorption behaviour. The pseudo-first-order model, pseudo-second-order kinetic model, Elovich model and intra-particle diffusion models were applied to the adsorption dynamic data. Pseudo-second-order fitted well in line with experimental data. Temkin adsorption isotherm best suited the adsorption data over the entire range of concentrations compared to other models.

Keywords: Biosorption; Reactive blue 19; Isotherm; Kinetics; Freshwater algae; Seaweed

1. Introduction

A variety of chemically different dyes are used for various industrial applications, such as textile dyeing, paper printing, leather, shoe polishing, plastics, food colouring, etc. The extensive use of dye often poses pollution problems in the form of coloured wastewater discharged into water bodies. Dye wastewaters discharged from textile and dyestuff industries have to be treated due to their impact on water bodies and growing public concern over their toxicity and carcinogenicity in particular [1]. Anthraquinone-based dyes are the most resistant to degradation due to their fused aromatic structures, which remain coloured for a longer period of time [2].

Several methods which include physico-chemical flocculation combined with flotation, electro flotation, flocculation with Fe(II)/$Ca(OH)_2$, membrane-filtration, electro kinetics coagulation, electrochemical destruction, ion-exchange, irradiation, precipitation, ozonation and the Katox treatment method have been employed for the treatment of dye containing wastewater [2–4]. All these methods have different colour removal capabilities, capital costs and operating rates [4]. However, most of the above methods are costly and suffer from one or more limitations and produce secondary pollutants. Adsorption techniques for wastewater treatment have become more popular in recent years owing to

*Corresponding author.

their efficiency in the removal of pollutants that are too stable for biological methods [5]. Biosorption has emerged as an alternative eco-friendly technology to remove dye from aqueous solutions.

Algae are photosynthetic organisms, which are distributed in nearly all parts of the world and in all kinds of habitats. Algae can degrade a number of dyes, postulating that the reduction appears to be related to the molecular structure of dyes and the species of algae used [6]. It is now recognized that the efficiency and the selectivity of adsorption by microbial biomass are due to the ion-exchange mechanism. Dead cells of tested genera showed a higher uptake than living cells due to an increased surface area. The mode of solute uptake by dead/inactive cells is extracellular, and the chemical functional groups of the cell wall play vital roles in biosorption [7].

Algal biomasses contain a variety of functional groups, such as carboxyl, hydroxyl, sulphate, phosphate and other charged groups. The totality of these groups is not accessible in the biomass natural form. This manner, the preparation of the micro particles from biomass is a good way to increase the accessible biosorption sites of the biomass [8].

Reactive Blue 19 dye is an anthraquinone-based vinyl sulphone dye. It is used in dyeing of cellulosic fibres [9]. In the particular case of the Reactive Blue 19, the relatively low fixation efficiency (75–80%) is due to the competition between the formation of the reactive form (vinyl sulfone) and the hydrolysis reactions [10]. Without adequate treatment, the dye may be stable and remain in the environment for a longer time. Due to chemical stability and low biodegradability of RB-19, a wide range of methods have been developed for their removal from waters and wastewaters to decrease their impact on the environment. The comparison of physio-chemical and biological treatment of RB 19 dye suggested that the degradation of dyes is an efficient and cost-effective process [9].

In this work, the potential of dead biomass of *Spirulina platensis* and *Gracilaria edulis* as biosorbents for removal of the synthetic dye (Reactive Blue 19) was investigated by varying some parameters, such as solution pH, initial dye concentration, contact time, adsorbent dosage, agitation speed, particle size and temperature.

2. Materials and methods

2.1. Dyestuff and aqueous solution

The reactive blue 19 (RB 19) used in this study, whose structure is shown in Fig. 1, was procured from Sigma–Aldrich chemical company (Bangalore, India)

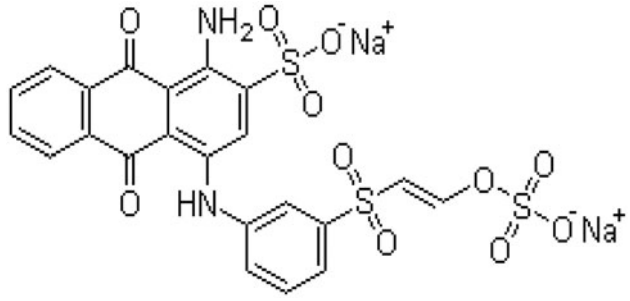

Fig. 1. Chemical structure of RB 19.

and was further used without any purification. All the used chemicals were of analytical grade. The stock dye solution was prepared by dissolving 1 g of RB 19 in 1 L of deionized water. The other required concentrations were prepared by diluting the stock solution of RB19. Fresh dilutions were used for each experiment. The pH of the working solutions was adjusted using 0.1 N HCl or 0.1 N NaOH. The properties of the dye are shown in Table 1.

2.2. Sorbent

The *S. platensis* was collected from the pond in Annamalainagar, Chidambaram. The seaweed *G. edulis* was collected from Mandapam, Rameshwaram. Then it was extensively washed several times with tap water and then with deionized water to remove dirt and small aquatic organisms. Afterwards, it was dried at room temperature for 24 h. The algal samples were ground and sieved to different particle sizes and subsequently used for sorption experiments.

2.3. Sorption experiment

Batch adsorption experiments were carried out to investigate the sorption of reactive dye on biosorbents. Exactly 100 ml of dye solution of known initial concentration (100 mg/L) was shaken at the certain agitation speed (150 rpm) with a required dose of adsorbents (1.0 g/L) for a specific period of contact time (300 min) in an orbital shaker, after noting down the initial pH

Table 1
Details of dye

Dyestuff name	Reactive blue 19 (RB 19)
Colour index number	61,200
Formula	$C_{22}H_{16}N_2Na_2O_{11}S_3$
Molecular weight	626.54
λ_{max}	592 nm

of the solution to the optimum pH at room temperature (30 ± 2 ℃). The final concentration (C_o) was measured.

The concentration in the test solution was determined spectrophotometrically using a UV Double beam spectrophotometer, (HITACHI U-2001) at a wavelength corresponding to the maximum absorbance (592 nm).

The percentage removal of dye was calculated using the following relationship:

$$\text{Removal efficiency}(\%) = \frac{C_i - C_o}{C_i} \times 100 \quad (1)$$

where C_i and C_o (both in mg/L) are the initial dye concentration and the dye concentration at any time, respectively.

The adsorption capacity q_t (mg/g) at any time was calculated using the mass balance relationship equation as follows:

$$q_t = (C_i - C_o) \times \left(\frac{V}{m}\right) \quad (2)$$

where V is the volume of the solution (L) and m is the mass of the dry adsorbent used (g).

2.4. Adsorption isotherm

Adsorption isotherm is the basic requirement for designing any adsorption system. Isotherm expresses the relation between the amounts of adsorbate removed from the liquid phase by unit mass of adsorbent at constant temperature. Since adsorption is one of the fundamental surface phenomena, it is important to have a satisfactory description of an equilibrium state in order to successfully represent the kinetic adsorption behaviour of any species from the fluid to the solid phase. The Langmuir, Freundlich, Dubinin–Radushkevich and Temkin adsorption isotherms were employed to determine the preference of one to another.

Langmuir adsorption isotherm, originally developed to describe gas–solid phase adsorption onto activated carbon, has traditionally been used to quantify and contrast the performance of different biosorbents [11]. The non-linear and linear forms of Langmuir isotherm is represented by Eqs. (3) and (4):

$$q_e = \frac{q_{\max} k_L C_e}{1 + k_L C_e} \quad (3)$$

$$\frac{1}{q_e} = \frac{1}{q_{\max}} + \frac{1}{k_L q_{\max} C_e} \quad (4)$$

The values of $q_{\max}$ and k_L can be determined from the slope ($1/q_{\max}$) and intercept ($1/k_L q_{\max}$) of the linear plot of $1/q_e$ vs. $1/C_e$. The Langmuir equation is used for homogeneous surfaces.

Freundlich sorption isotherm is the most commonly used empirical expression describing the sorption from solutions and deals with surface heterogeneity, exponential distribution of active sites of sorbent and their energies towards sorbate [12]. The non-linear and linear forms of Freundlich isotherm are represented by Eqs. (5) and (6):

$$q_e = K_F C_e^{1/n} \quad (5)$$

$$\log\ q_e = \log\ K_F + \frac{1}{n} \log\ C_e \quad (6)$$

The values of K_F and n can be determined from the slope ($1/n$) and intercept ($\log K_F$) of the linear plot of $\log q_e$ vs. $\log C_e$.

Dubinin—Radushkevich isotherm model [13] is postulated within a sorption space close to the sorbent surface to evaluate the sorption free energy and help to determine the nature of bonding either physisorption (or) chemisorptions [14]. The non-linear and linear forms of D–R isotherm are represented by Eqs. (7) and (8):

$$q_e = q_s \exp(-k_{ad}\varepsilon^2) \quad (7)$$

$$\ln q_e = \ln\ (q_s) - k_{ad}\varepsilon^2 \quad (8)$$

Polanyi potential (ε) is given as the Eq. (9):

$$\varepsilon^2 = \text{RT}\ \ln\left(1 + \frac{1}{C_e}\right) \quad (9)$$

The values of q_s and k_{ad} can be determined from the slope ($-K_{ad}$) and intercept ($\ln q_s$) of the linear plot of $\ln (q_e)$ vs. ε^2.

This isotherm contains a factor that explicitly takes into account the adsorbent–adsorbate interactions. By ignoring the extremely low and large value of concentrations, the model assumes that the heat of adsorption (function of temperature) of all molecules in the layer would decrease linearly rather than logarithmic with coverage [15]. The non-linear and linear

forms of Temkin isotherm are represented by Eqs. (10) and (11):

$$q_e = \frac{\mathrm{RT}}{B_t} \ln A_t C_e \tag{10}$$

$$q_e = \frac{\mathrm{RT}}{B_t} \ln A_t + \left(\frac{\mathrm{RT}}{B_t}\right) \ln C_e \tag{11}$$

The values of A_t and B_t can be determined from the slope RT/B_t and intercept (RT/B_t) ln A_t of the linear plot of q_e vs. ln C_e.

2.5. Adsorption kinetics

Kinetic models are widely used for interpreting the dynamic interaction between adsorbent and adsorbate. Also, to find the potential rate-controlling steps involved in the process of adsorption of RB 19 onto biosorbents, the pseudo-first-order, pseudo-second-order rate equation, Elovich model and intra-particle diffusion kinetic models were tested to fit the experimental data.

The sorption kinetics may be described by a Lagergren's pseudo-first-order model [16]. The differential equation is the following:

$$\frac{dq_t}{dt} = k_1(q_e - q_t) \tag{12}$$

Integrating Eq. (12) for the boundary conditions $t = 0$ to $t = t$ and $q_t = 0$ to $q_{t\,=}\, q_t$, gives:

$$\log \frac{q_e}{q_e - q_t} = \left(\frac{k_1}{2.303}\right) t \tag{13}$$

This is the integrated rate law for a pseudo-first-order reaction.

Eq. (13) can be rearranged to obtain a linear form:

$$\log (q_e - q_t) = \log (q_e) - \left(\frac{k_1}{2.303}\right) t \tag{14}$$

In order to obtain the rate constants, the straight line plots of log (q_e − q_t) against t for different dyes and different experimental conditions have been analysed.

The sorption kinetics may be described by a Ho's pseudo-second-order model [17]. The differential equation is the following:

$$\frac{dq_t}{dt} = k_2(q_e - q_t)^2 \tag{15}$$

Integrating Eq. (15) for the boundary conditions $t = 0$ to $t = t$ and $q_t = 0$ to $q_t = q_t$, gives:

$$\frac{1}{(q_e - q_t)} = \frac{1}{q_t} + k_2 t \tag{16}$$

This is the integrated rate law for a pseudo-second-order reaction. Eq. (16) can be rearranged to obtain a linear form:

$$\frac{t}{q_t} = \frac{1}{k_2 q_e^2} + \frac{1}{q_e t} \tag{17}$$

The straight line plots of t/q_t against t have also been tested to obtain rate parameters (k_2 and q_e).

The rate of intra-particle diffusion is a function of $t^{0.5}$ and can be defined by Eq. (18) as follows [18]:

$$q_t = k_{id} t^{0.5} + I \tag{18}$$

where k_{id} is the intra-particle diffusion rate constant. The k_{id} values were calculated from the slopes of the straight line portions of the respective plots. If intra-particle diffusion is a rate-controlling step, then the plots should be linear and pass through the origin.

The Elovich equation is mainly applicable for chemisorption kinetics. The equation is often valid for systems in which the adsorbing surface is heterogeneous [19]. The kinetics of adsorption can also be described by the Elovich model [20,21]. The Elovich equation is as follows:

$$\frac{dq_t}{dt} = a \exp\,(-bq_t) \tag{19}$$

Integrating Eq. (19) with the conditions $q_t = 0$ at $t = 0$; $q_t = q_t$ at $t = t$ and subsequently linearizing the integrated equation result in:

$$q_t = \left(\frac{1}{b}\right) \ln\,(ab) + \left(\frac{1}{b}\right) \ln\,(t + t_0) \tag{20}$$

where a and b are the parameters of the Elovich rate equation; t_0 is equal to 1/(ab). If abt>>1, Eq. (20) can further be simplified as:

$$q_t = \left(\frac{1}{b}\right) \ln\,(ab) + \left(\frac{1}{b}\right) \ln t \tag{21}$$

A plot of q_t vs. ln t yields a linear relationship with a slope of (1/b) and an intercept of 1/b ln (ab).

3. Results and discussion

3.1. Effect of pH

The effect of initial pH on the adsorption of RB19 onto *S. platensis* and *G. edulis* biomasses were studied, while the initial dye concentration, shaking time, amount of sorbent and temperature were fixed at 100 mg/L, 300 min, 0.20 g and 30 ℃, respectively. Sorption of dye highly depends upon the solution pH. Maximum uptake was at pH 1.5 in both cases with comparatively little uptake occurring between pH 3 and 7, after pH 7, a small increase in adsorption was observed (Fig. 2). The enhancement of uptake of reactive dyes at acidic pH may be explained in terms of electrostatic interactions between the biomass and the dye particles [22]. It seems that the rate of dissociation of the dyes as well as the ionization of the cationic substrate dominates in the acidic medium. Decrease in the dye adsorption capacity with increasing pH may be due to the positive charge on the oxide or solution surface appears negatively charged OH^- ions and the facilities lead to ionic repulsion between the negatively charged surface and the anionic dye molecules. The maximum adsorption capacity of RB 19 takes place at around acidic pH 1.5. A similar result of pH effect was also reported for the adsorption of RB 19 dye onto modified bentonite [23].

3.2. Effect of sorbent dosage

The effect of the dosage of *S. platensis* sand *G. edulis* biomasses on the amount of dye adsorbed was studied by agitating 100 ml of 100 mg/L of dye solution with different amounts of sorbents, namely 0.1, 0.2, 0.3, 0.4 and 0.5 g. All these studies were conducted at room temperature at a constant agitation speed of 150 rpm. Fig. 3 shows the effect of adsorbent dosage on the amount of dye adsorbed q_e (mg/g) and it was observed that the amount of dye adsorbed varied with initial adsorbent dosage. The dye uptake decreased from 96.9 to 19.7 mg/g (*S. platensis*) and 82.3 to 17.72 mg/g (*G. edulis*) for an increase in sorbent dosage of 0.1 to 0.5 g. The maximum dye uptake was obtained at the sorbent dosage of 1.0 g/L. An increase in dye uptake was observed to decrease in adsorbent dosage. This may be due to the active surface area of the unit mass of sorbent decreased due to the aggregation or overlapping of biomass particles [24,25]. A similar result of the sorbent dose effect was also reported for the removal of Malachite green by *Turbinaria conoides* as biosorbent [26].

3.3. Effect of temperature

The influence of temperature on the sorption of RB 19 by the *S. platensis* and *G. edulis* biomasses was studied with a temperature range of 30, 35, 40, 45 and 50 ℃. The temperature profile (Fig. 4) indicates that as the temperature increases the sorption capacity decreases. This is because the biosorbent loses its properties at very high temperatures due to denaturation. The maximum sorption capacity was attained at 30 ℃ for both sorbents. The similar phenomena were observed by the biosorption of synthetic dyes from aqueous solution by *S. platensis* nanoparticles [8].

3.4. Effect of agitation speed

Agitation rate plays an important role in the adsorption process [27] and the effect of agitation speed on the adsorption capacity of both freshwater algae and seaweed was studied by varying the shak-

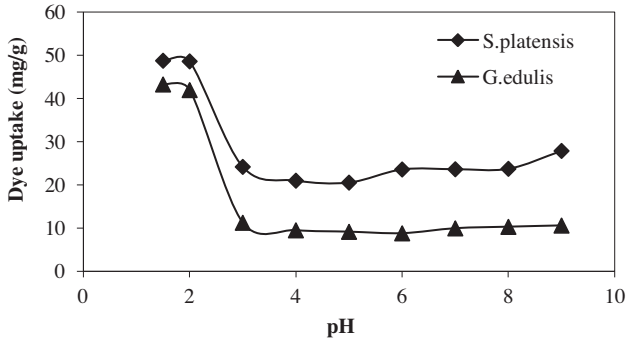

Fig. 2. Effect of pH on sorption of RB 19 by *S. platensis* and *G. edulis* biomasses (initial dye concentration—100 mg/L, sorbent dose—0.2 g/100 ml, agitation speed—150 rpm and temperature—30 ℃).

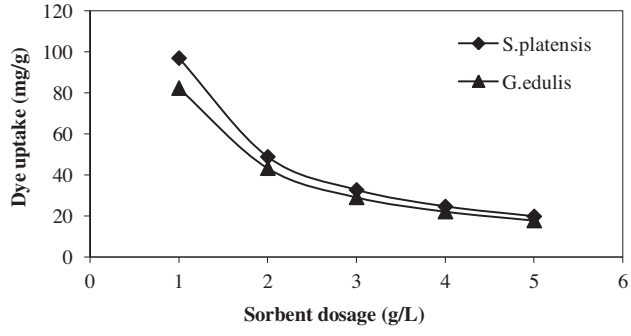

Fig. 3. Effect of sorbent dose on sorption of RB 19 by *S. platensis* and *G. edulis* biomasses (pH—1.5, initial dye concentration—100 mg/L, agitation speed—150 rpm and temperature—30 ℃).

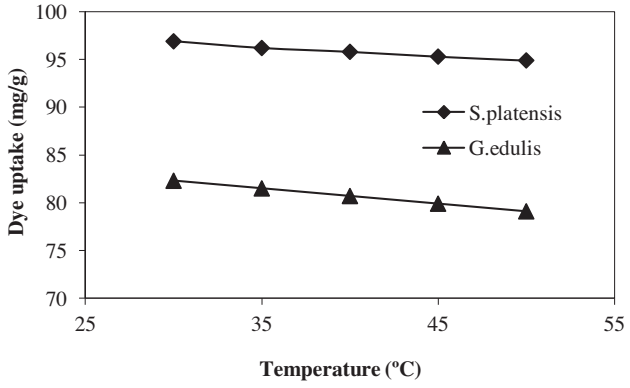

Fig. 4. Effect of temperature on sorption of RB 19 by *S. platensis* and *G. edulis* biomasses (pH—1.5, initial dye concentration—100 mg/L, sorbent dose—0.1 g/100 ml and agitation speed—150 rpm).

ing speeds (25, 50, 100, 150 and 250 rpm). The influence of agitation speed on adsorption of dye is shown in Fig. 5. The amount adsorbed at equilibrium was found to increase with increase in agitation speed from 25 to 150 rpm. This is due to the change in boundary layer resistance of the system. The boundary layer resistance will be affected by the rate of adsorption and increasing the degree of agitation will reduce this resistance and increase the mobility of the system, due to this the adsorbate molecules are forced towards the surface of the adsorbate [28,29]. The maximum uptake of RB 19, 96.9 and 82.3 mg/g was obtained at 150 rpm by *S. platensis* and *G. edulis*, respectively. Though the shaking speed rose above 150 rpm, diffusion speeds decreased. This decrease in uptake capacity may be attributed to an increase desorption tendency of dye molecules and/or having a similar speed of adsorbent particles and adsorbate ions (i.e. the formation of a more stable film around the adsorbent particles). This desorption tendency may be attributed to a high mixing speed, which means additional energy input and higher shear force cause a break in newly formed bonds between the dye and the adsorbent [30]. Thus, the optimum agitation speed was selected as 150 rpm.

3.5. Effect of sorbent particle size

The consequence of sorbent particle size (<75, 75–150, 150–300, 300–600, >600 μm) on biosorption of dye is shown in Fig. 6. The maximum dye uptake was obtained for the particle size of < 75 μm for both sorbents. The dyes adsorbed increased as the sorbent particle size decreased. The increase in sorption depends on the vast external surface area of small particles. It is well known that decreasing the average particle size of the adsorbent increases the surface area, which in turn increases the adsorption capacity [31]. The same trend of adsorbent size effect was also reported for the biosorption of Cationic dyes using Granulized *Annona squmosa* Seed [32].

3.6. Effect of contact time

The contact time between the dye molecules and the sorbent is significant in the dye treatment by sorption. The effect of contact time on the sorption of RB 19 was studied at a sorbent dose of 0.10 g, a solution volume of 100 ml, an agitation speed of 150 rpm and a temperature of 30 ˚C for various dye concentrations of 50, 100, 150, 200 and 250 mg/L. The effect of contact time on the removal of dye by the studied sorbents is shown in Figs. 7 and 8. The percentage sorption of dye uptake was rapid in the first 30 min, then the rate drastically

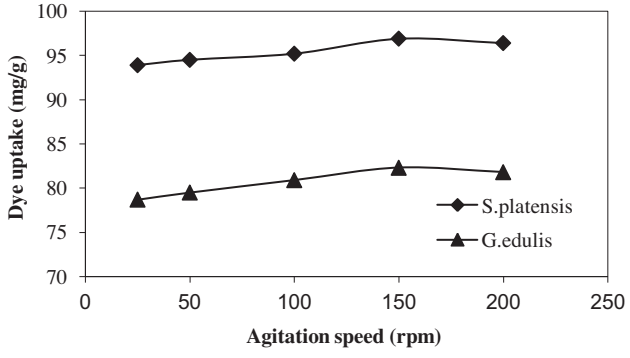

Fig. 5. Effect of shaking speed on sorption of RB 19 by *S. platensis* and *G. edulis* biomasses (pH—1.5, initial dye concentration—100 mg/L, sorbent dose—0.1 g/100 ml and temperature—30 ˚C).

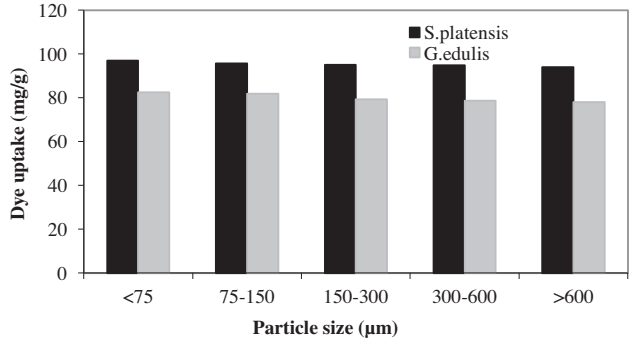

Fig. 6. Effect of particle size on sorption of RB 19 by *S. platensis* and *G. edulis* biomasses (pH—1.5, initial dye concentration—100 mg/L, sorbent dose—0.1 g/100 ml, temperature—30 ˚C and agitation speed—150 rpm).

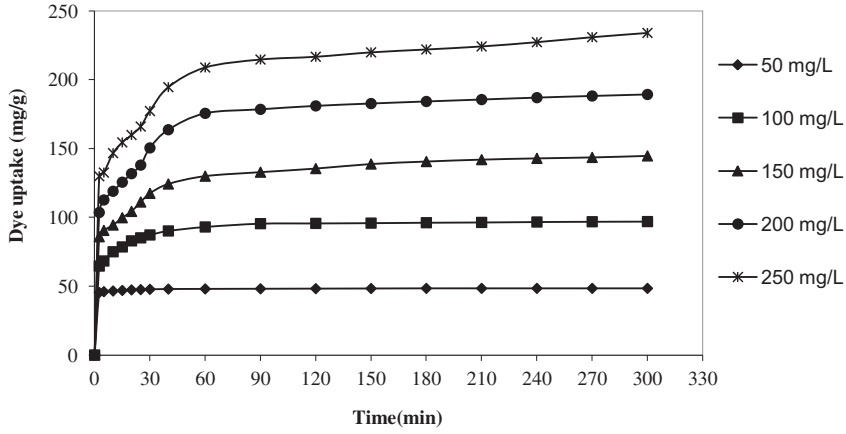

Fig. 7. Effect of contact time on sorption of RB 19 by *S. platensis* biomass (pH—1.5, initial dye concentration—100 mg/L, sorbent dose—0.1 g/100 ml, temperature—30 ℃ and agitation speed—150 rpm).

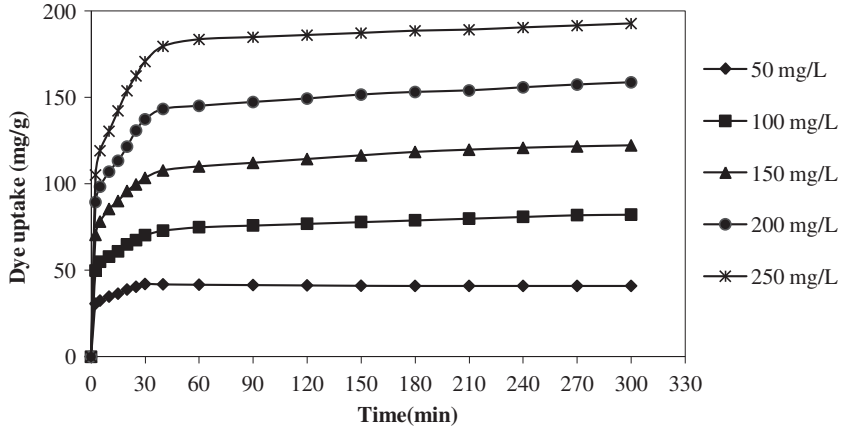

Fig. 8. Effect of contact time on sorption of RB 19 by *G. edulis* biomass (pH—1.5, initial dye concentration—100 mg/L, sorbent dose—0.1 g/100 ml, temperature—30 ℃ and agitation speed—150 rpm).

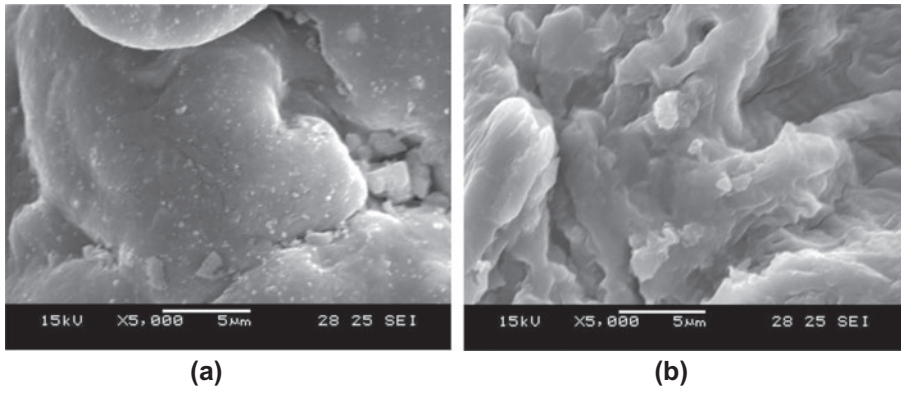

Fig. 9. Scanning electron micrographs of (a) *S. platensis* and (b) dye-loaded *S. platensis*.

decreased and eventually approached almost zero, ultimately the equilibrium point had reached. These changes in the rate of removal may be due to the fact that, initially all adsorbent sites are vacant and the solute concentration gradient is high. The decrease in the rate with time indicates the slow approach to equilibrium possibly by internal diffusion [33]. Also the equilibrium time increased with increase in initial dye concentration. The dye solution of concentration 50 mg/L attained the equilibrium condition within 180 min. But for 100 mg/L dye solution, the contact time needed to reach equilibrium is about 300 min. At this point, the sorbed amount of dye by biomass is in a state of dynamic equilibrium with the amount of the dye desorbing from the sorbent. In the adsorption progress, initially the dye molecules first encountered the boundary layer effect and then diffused from the boundary layer film onto the sorbent surface and finally, they diffused into the porous structure of the sorbent [25]. Therefore, the dye solution with higher initial dye concentration will take relatively longer time to reach equilibrium due to higher amount of dye molecules. Thus, the optimum contact time for batch sorption was chosen as 300 min. A similar result of the contact time effect was also reported for the adsorption of Reactive dyes onto the bagasse fly ash [34].

3.7. Effect of initial dye concentration

The effect of initial dye concentration on the adsorption of RB19 onto *S. platensis* and *G. edulis* biomasses was studied, while the pH, shaking time, amount of sorbent and temperature were fixed at 1.5, 300 min, 0.1 g and 30 ℃, respectively. Batch experiments were carried out by agitating 100 ml of dye solutions with concentrations of 50, 100, 150, 200 and 250 mg/L. The amount of dye adsorbed increased with the increase of initial dye concentration. Increasing the initial dye concentration increases the mass gradient between the solution and the adsorbent, and therefore, the rate at which dye molecules pass from the bulk solution to the particle surface and the amount of transfer at equilibrium [35].

3.8. SEM and FTIR measurement

3.8.1. Scanning electron micrograph images

The surface of adsorbents was characterized by scanning electron microscopy (SEM, Jeol JSM 60) before and after the adsorption experiments for *S. platensis* (Fig. 9) and *G. edulis* (Fig. 10). The SEM image (magnification ×5000) clearly shows that the morphological changes occur after adsorption. It is clear that the dye has been adsorbed on the active sites of the adsorbent.

3.8.2. FTIR measurement

FTIR technique was used to examine the surface groups of the adsorbent and to identify those groups responsible for dye adsorption. The FTIR spectra of the samples were recorded on Perkin Elmer FTIR spectrophotometer (Spectrum BX-II) using a pellet (pressed-disk) technique. For this, the adsorbent was intimately mixed with approximately 100 mg of dry, powdered KBr. The infrared spectra of sorbents *S. platensis* (Fig. 11), *G. edulis* (Fig. 12) and dye-loaded sorbent samples were recorded in the range 4,000–400 cm^{-1}.

Adsorption peak at 3424.23 cm^{-1} in *S. platensis* (Fig. 11), indicates the N–H stretching vibration due to the presence of secondary amines (protein, lipid). The Aliphatic C–H stretching vibration can be observed at 2923.12 and 2860.27 cm^{-1}. The adsorption bands at

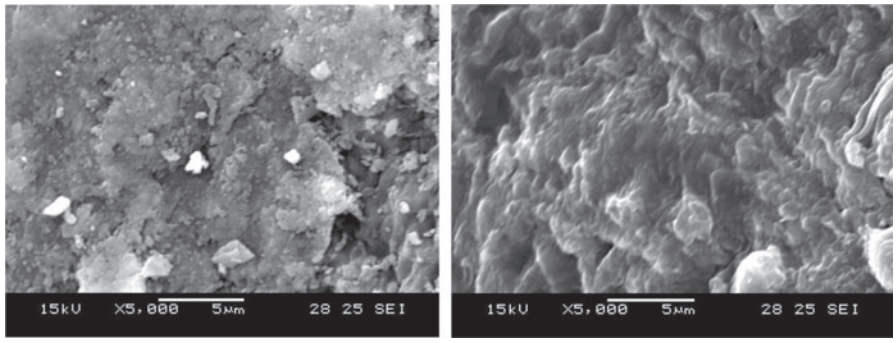

Fig. 10. Scanning electron micrographs of (a) *G. edulis* and (b) dye-loaded *G. edulis*.

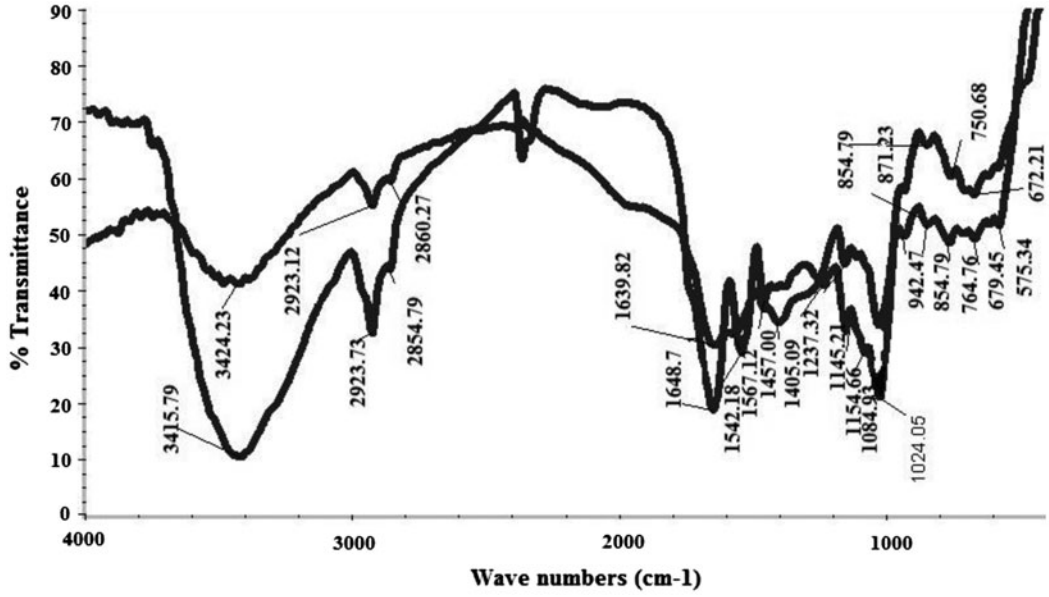

Fig. 11. FTIR spectra of *S. platensis* and dye-loaded *S. platensis*.

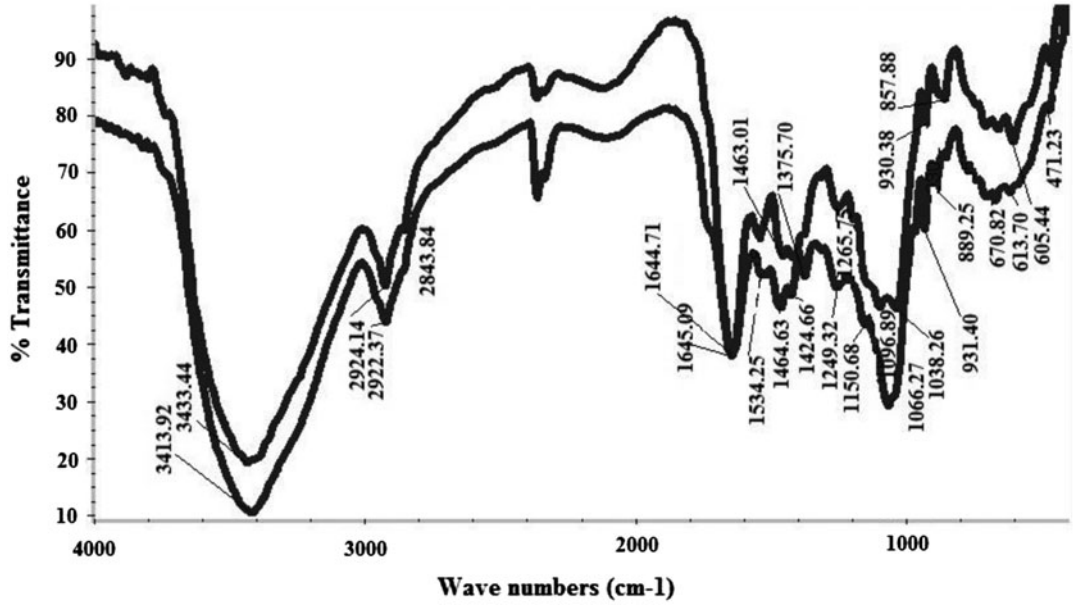

Fig. 12. FTIR spectra of *G. edulis* and dye-loaded *G. edulis*.

1639.82 and 1567.12 cm^{-1} are assigned to N–H bending vibration present in the Carbonyl β-Unsaturated Ketone amide. The bending of NH_4^+ and bending of CH_2 were identified at wave numbers 1463.01 and 1405.09 cm^{-1}. The peak acquired at 1024.73 cm^{-1} is due to C–H and SO_3 symmetric stretching. The S–O stretching was identified at 679.45 cm^{-1}. The FTIR spectra shown in Fig. 11 clearly indicate that the complex formation has been occurring between *S. platensis* and RB-19 dye, which is evident from shifting of the band at 3,424 to 3,415 cm^{-1}. Thus, the vanishing of older and appearance of other new bands in FT-IR spectra are clear indications of chemical interaction between the dyes and sorbent.

Peak in the wave number 1265.75 cm^{-1} in *G. edulis* (Fig. 12), shows the presence of the C–O–C bond.

Several peaks were obtained in the region of 1,500–500 cm^{-1} indicated the vibrational modes that are specific to the type of polysaccharides and glycosidic linkages. Also it denotes the presence of aldehyde functional groups which are actively involved in biosorption. Amide I bands are (1700–1600 cm^{-1}) due to C=O stretching vibrations of peptide bond provide insight into the protein secondary structure. Similar peaks were obtained at 1644.71 cm^{-1}.

3.9. Adsorption isotherm

The results showed that the Langmuir, Freundlich, D–R model and Temkin models were, moreover, suitable for describing the adsorptions on sorption of RB 19 by *S. platensis* and *G. edulis* biomasses. Figs. 13 and 14 represent the different adsorption isotherms along with the experimental data for *S. platensis* and *G. edulis* biomasses, respectively.

The R^2 value is 0.996, proving that the sorption data fitted well to Langmuir Isotherm model for *G. edulis*. The maximum dye uptake (q_{max}, 909.09 mg/g) on *G. edulis* is about two times larger than that of *S. platensis*. This may be due to the inherent properties of biomass. In freundlich isotherm, the values of n lie between 1 and 10 indicating favourable adsorption.

Table 2 shows that the equilibrium data fit better with Temkin isotherm over the entire range of concentrations compared to Langmuir, Freundlich and D-R models. Also the highest correlation coefficient (R^2 = 0.994) value (Table 2) shows that Temkin isotherm gave very good fit to the adsorption data for *S. platensis*. From Table 2, A_t (Temkin) value of *S. platensis* is larger than that of *G. edulis*. This means that the absorbent/adsorbate interaction of *S. platensis* is larger than that of *G. edulis*.

Among all these isotherms, Dubinin–Radushkevich isotherm was given the poor fit to the experimental

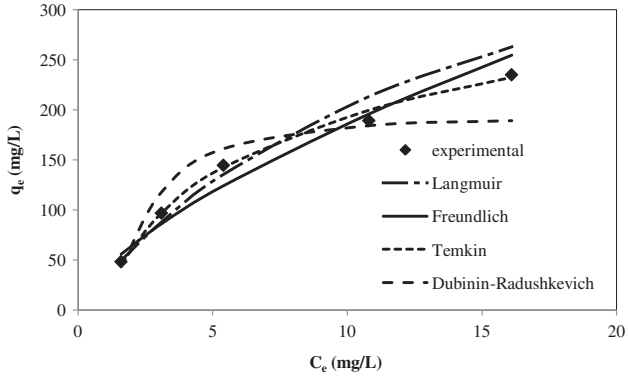

Fig.13. Isotherm plot for RB 19 adsorption on *S. platensis*.

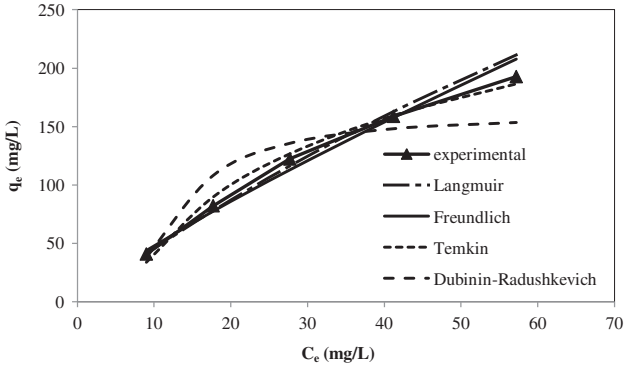

Fig. 14. Isotherm plot for RB 19 adsorption on *G. edulis*.

adsorption equilibrium data of *S. platensis* (R^2 = 0.930) and *G. edulis* (R^2 = 0.902).

3.10. Adsorption kinetics

Adsorption kinetics of RB 19 by pseudo-first-order model, pseudo-second-order model, intra-particle diffusion model and Elovich model were plotted and Table 3 shows the kinetic constants and correlation coefficients of the models. Fig. 15 shows the kinetics plots of adsorption of RB 19 on to *S. platensis* and *G. edulis*.

3.10.1. Pseudo-first-order model

It can be seen that, from the rate constants and correlation coefficient values (Table 3) of pseudo-first-order model, the adsorption did not obey well with the pseudo-first-order model because of the absence of linearity between log ($q_e - q_t$) and t. According to Eq. (14), a plot of log ($q_e - q_t$) against t should give a straight line to confirm the applicability of the kinetic model. In a true first-order process, log q_e should be equal to the intercept of a plot of log ($q_e - q_t$) against t. From the results in Table 3, it is observed that the theoretical values (q_e, cal) were much lower than those of the experimental data (q_e, exp) and low correlation coefficient values obtained for the pseudo-first-order model indicated that sorption does not occur exclusively on one site per ion [36].

3.10.2. Pseudo-second-order model

In this study, the pseudo-second-order model fitted well when compared with pseudo-first-order model. Therefore, the adsorption data in this study supported the chemisorptions. The values of q_e calculated by the pseudo-second-order equation are also in good

Table 2
Isotherm constants and their coefficients for RB 19 adsorption onto *S. platensis* and *G. edulis*

Isotherm	Constants/R^2	*S. platensis*	*G. edulis*
Langmuir	q_{max} (mg/g)	500	909.09
	K_L (L/mg)	0.0689	0.00532
	R^2	0.988	0.996
Freundlich	K_F (mg/g)	41.0	6.934
	n	1.522	1.19
	R^2	0.958	0.986
Dubinin–radushkevich	q_s (mg/g)	193.64	159.49
	k_{ad}	1.0×10^{-6}	2.03×10^{-5}
	R^2	0.930	0.902
Temkin	A_t (L/mg)	1.126	0.168
	B_t	31.935	30.59
	R^2	0.994	0.988

Table 3
Kinetic constants and their coefficients for RB 19 adsorption onto *S. platensis* and *G. edulis*

Kinetic model	Constants/R^2	*S. platensis*	*G. edulis*
Pseudo-first-order model	q_e (mg/g) exp	233.9	192.8
	q_e (mg/g) cal	98.62	53.08
	k_1 (1/min)	0.0115	0.0138
	R^2	0.927	0.881
Pseudo-second-order model	q_e (mg/g) exp	233.9	192.8
	q_e (mg/g) cal	250	200
	k_2 (g/mg min)	5.517×10^{-4}	1.315×10^{-3}
	R^2	0.998	0.999
Intra-particle diffusion model	$k_{id\ 1}$ (mg/g $min^{1/2}$)	13.45	13.63
	I_1	103.6	89.31
	R^2	0.981	0.955
	$k_{id\ 2}$ (mg/g $min^{1/2}$)	2.457	0.951
	I_2	189.8	175.8
	R^2	0.984	0.991
Elovich model	a (mg/g/min)	1211.96	3604.72
	b (g/mg)	0.0408	0.055
	R^2	0.965	0.918

agreement with the experimental data (q_e, exp), as shown in Table 3.

3.10.3. Intra-particle diffusion study

In the present study, the linear plot of q_t vs. $t^{0.5}$ was not passing through the origin. The deviation of these lines from the origin indicates that intra-particle transport is not a rate-limiting step. It can be assumed that external mass transfer controls the rate of adsorption because of the very slow transfer speeds [28]. Further, such deviation of straight line from the origin indicates that the pore diffusion is not the sole rate-controlling step [37]. Intercept values (Table 3) give an idea about the thickness of the boundary layer, i.e. the larger the intercept, the greater is the boundary layer effect [38]. The first and sharper portion is attributed to the boundary layer diffusion of dye molecules. The second portion corresponds to the gradual adsorption stage, where intra-particle diffusion was a rate-limiting step [39]. The intra-particle diffusion model study indicated that the dye uptake process was found to be controlled by external mass transfer at first stages and by intra-particle diffusion at second stages [40]. So, the adsorption mechanism was suggested to be complex, consisting of both surface adsorption and pore diffusion.

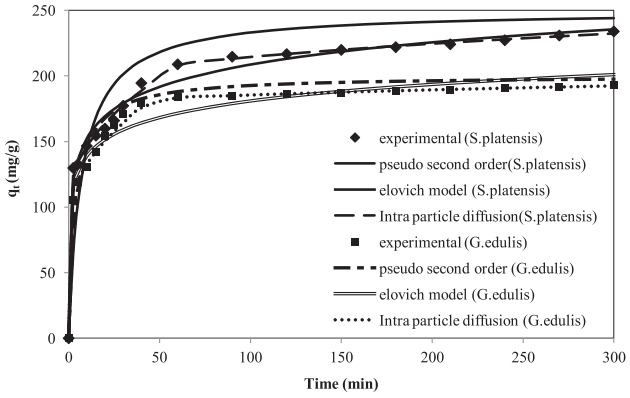

Fig. 15. Kinetics plot for RB 19 adsorption on *S. platensis* and *G. edulis*.

3.10.4. Elovich model

The Elovich rate equation is commonly used to describe the sorption behaviour with a rapid equilibrium rate in the early period, while it slows down the equilibrium at later periods of the sorption process [41]. The higher values of constant *a* for sorption of RB 19 on *S. platensis* implies higher chemisorptions rate than sorption of RB 19 on *G. edulis*. The correlation coefficient values obtained for the Elovich model implies that sorption provide the best fit for the adsorption of RB 19 onto *S. plantesis* and *G. edulis*.

4. Conclusions

In this work, the ability of sorbents *S. platensis* and *G. edulis*, cost effective and widely available biomasses on removal RB 19 from aqueous solution was investigated. The results obtained from the present investigation revealed that the ability of biomasses was efficient in removing Reactive dye from aqueous solution. The maximum adsorption capacity was obtained (96.9 and 82.3 mg/g) at a solution pH~1.5 by *S. platensis* and *G. edulis*, respectively. The optimum condition for the removal of RB 19 using both biomasses were found to be: temperature (30 ℃), adsorbent dose (1.0 g/L), contact time (300 min), adsorbent size (≤75 μm) and agitation speed (150 rpm). Various isotherms used to observe the adsorption behaviour were Langmuir, Freundlich, Dubinin–Radushkevich and Temkin. Equilibrium adsorption data for RB 19 on *S. platensis* were best represented by the Temkin isotherm and Equilibrium isotherms were well described by the Langmuir equation, giving maximum adsorption capacity of *G. edulis* 909.09 mg/g at 30 ℃. Among the kinetic models (Lagergren's pseudo-first-order model, pseudo-second-order model, Elovich model and the intra-particle diffusion model), the adsorption kinetics can be well described by the pseudo-second-order model equation and followed by the intra-particle diffusion as one of the rate-determining steps.

Acknowledgments

The authors wish to convey their gratefulness for the support extended by the authorities of the Annamalai University, Annamalai Nagar, India, in carrying out the research work in Environmental Engineering Laboratory, Department of Civil Engineering.

Nomenclature

- a — Elovich rate equation constant representing initial rate of sorption (mg/g/min);
- A_T — Temkin isotherm equilibrium binding constant (L/g).
- b — Elovich rate equation constant representing the extent of surface coverage and the activation energy of chemisorption (g/mg).
- B_T — Temkin isotherm constant.
- C_o — initial concentration of dye in solution (mg/L).
- C_e — equilibrium (residual) concentration of adsorbate in solution (mg/L).
- ε — Dubinin–Radushkevich isotherm constant.
- k_1 — the equilibrium rate constant of pseudo-first-order sorption (min^{-1}).
- k_2 — the equilibrium rate constant of pseudo-second-order sorption (g/mg/min).
- K_{ad} — Dubinin–Radushkevich isotherm constant (mol^2/kJ^2).
- K_{id} — intraparticle diffusion rate constant (mg/g-$min^{0.5}$).
- K_L — Langmuir isotherm constant (L/mg).
- K_F — Freundlich isotherm constant (mg/g).
- m — mass of the dry adsorbent used (g).
- n — adsorption intensity.
- q_e — amount of dye adsorbed per gram of the adsorbent at equilibrium (mg/g).
- q_{max} — maximum monolayer coverage capacity (mg/g).
- q_s — theoretical isotherm saturation capacity (mg/g).
- q_t — amount of dye sorbed at time t (mg/g).
- R — universal gas constant (8.314 J/mol/K).
- R^2 — correlation coefficient.
- t — sorption contact time (min).
- t_0 — 1/(*ab*) (1/min).
- T — temperature (K).
- V — volume of the solution (L).

References

[1] Y. Fu, T. Viraraghavan, Column studies for biosorption of dyes from aqueous solutions on immobilised *Aspergillus niger* fungal biomass, Water SA 29(4) (2003) 465–472.

[2] I.M. Banat, P. Nigam, D. Singh, R. Marchant, Microbial decolorization of textile-dyecontaining effluents: A review, Bioresour. Technol. 58 (1996) 217–227.
[3] R. Rajeshkannan, M. Rajasimman, N. Rajamohan, B. Sivaprakash, Equilibrium and kinetic studies on sorption of Malachite green using *Hydrilla Verticillata* biomass, Int. J. Environ. Res. 4(4) (2010) 817–824.
[4] G.O.E. Sayed, T.Y. Mohammed, O.E.E. Sayed, Removal of basic dyes from aqueous solutions by sugar can stalks, Adv. Appl. Sci. Res. 2(4) (2011) 283–290.
[5] S.J. Allen, B. Koumanova, Decolourisation of water/wastewater using adsorption (review), J. Chem. Technol. Metall. 40(3) (2005) 175–192.
[6] N. Daneshvar, M. Ayazloo, A.R. Khataee, M. Pourhassan, Biological decolorization of dye solution containing Malachite green by microalgae *Cosmarium* sp., Bioresour. Technol. 98 (2007) 1176–1182.
[7] A. Srinivasan, T. Viraraghavan, Decolorization of dye wastewaters by biosorbents: A review, J. Environ. Manage. 91 (2010) 1915–1929.
[8] G.L. Dotto, E.C. Lima, L.A.A. Pinto, Biosorption of food dyes onto *Spirulina platensis* nanoparticles: Equilibrium isotherm and thermodynamic analysis, Bioresour. Technol. 103 (2012) 123–130.
[9] M. Siddique, R. Farooq, A. Shaheenj, Removal of reactive blue 19 from wastewaters by physicochemical and biological processes—A review, Chem. Soc. Pak. 33(2) (2011) 284–293.
[10] R. Pelegrini, P.P. Zamora, A.R de Andrade, J. Reyes, N. Duran, Electrochemically assisted photocatalytic degradation of reactive dyes, *Appl. Catal. B: Environ.* 22 (1999) 83–90.
[11] I. Langmuir, The constitution and fundamental properties of solids and liquids, J. Am. Chem. Soc. 38(11) (1916) 2221–2295.
[12] H.M.F. Freundlich, Over the adsorption in solution, J. Phys. Chem. 57 (1906) 385–470.
[13] M.M. Dubinin, L.V. Radushkevich, The equation of the characteristic curve of activated charcoal, Proc. Acad. Sci. USSR Phys. Chem. Sect. 55 (1947) 331–337.
[14] R. Hemalatha, R. Chitra, X.R. Rathinam, P.N. Sudha, Synthesizing and characterization of chitosan graft co polymer: Adsorption studies for Cu(II) and Cr(VI) (2011), Int. J. Environ. Sci. 2(2) (2011) 805–828.
[15] M.I. Temkin, V. Pyzhev, Kinetics of ammonia synthesis on promoted iron catalyst, Acta Phys. Chim. USSR 12 (1940) 327–356.
[16] S. Lagergren, About the theory of so-called adsorption of soluble substances, K. Sven. Vetenskapsakad. Handl. 24(4) (1898) 1–39.
[17] Y.S. Ho, G. McKay, Sorption of dye from aqueous solution by peat, Chem. Eng. J. 70 (1998) 115–124.
[18] W.J. Weberand J.C. Morris, Kinetics of adsorption on carbon from solution, J. Sanitary Eng. Div. Proc. Am. Soc. Civil Eng. 89 (1963) 31–59.
[19] Y.S. Ho, G. McKay, A comparison of chemisorption kinetic models applied to pollutant removal on various sorbents, Process Saf. Environ. Prot. 76 (1998) 332–340.
[20] S.H. Chien, W.R. Clayton, Application of Elovich equation to the kinetics of phosphate release and sorption on soils, Soil Sci. Soc. Am. J. 44 (1980) 265–268.
[21] D.L. Sparks, P.M. Jardine, Comparison of kinetic equation to describe potassium calcium exchange in pure and in mixed systems, Soil Sci. 138(2) (1984) 115–122.
[22] T.O. Mahony, E. Guibal, J.M. Tobin, Reactive dye biosorption by *Rhizopus arrhizus* biomass, Enzyme Microb. Technol. 31 (2002) 456–463.
[23] O Gok, A.S. Ozcan, A. Ozcan, Adsorption behavior of a textile dye of reactive blue 19 from aqueous solutions onto modified bentonite, Appl. Surf. Sci. 256 (2010) 5439–5443.
[24] Y. He, J.F. Gao, F.Q. Feng, C. Liu, Y.Z. Peng, S.Y. Wang, The comparative study on the rapid decolorization of azo, anthraquinone and triphenylmethane dyes by zero-valent iron, Chem. Eng. J. 179 (2012) 8–18.
[25] Q. Shi, J. Zhang, C. Zhang, W. Nie, B. Zhang, H. Zhang, Adsorption of basic violet 14 in aqueous solutions using KMnO4-modified activated carbon, J. Colloid Interface Sci. 343 (2010) 188–193.
[26] R. RajeshKannan, M. Rajasimman, N. Rajamohan, B. Sivaprakash, Brown marine algae *Turbinaria conoides* as biosorbent for Malachite green removal: Equilibrium and kinetic modeling, Front. Environ. Sci. Eng. China 4(1) (2010) 116–122.
[27] N.A.B. Rohaizar, N.B.A. Hadi, W.C. Sien, Removal of Cu (II) from water by adsorption on chicken eggshell, Int. J. Eng. Technol. 13 (2013) 40–45.
[28] M.E. Argun, S. Dursun, C. Ozdemir, M. Karatas, Heavy metal adsorption by modified oak sawdust: Thermodynamics and kinetics, J. Hazard. Mater. 141 (2007) 77–85.
[29] D.N. Jadhav, A.K. Vanjara, Adsorption kinetics study: Removal of dyestuff effluent using sawdust, polymerized sawdust and sawdust carbon-II, Ind. J. Chem. Technol. 11 (2004) 42–50.
[30] M.M.A. Latif, A.M. Ibrahim, M.F.E. Kady, Adsorption equilibrium, kinetics and thermodynamics of methylene blue from aqueous solutions using biopolymer oak sawdust composite, J. Am. Sci. 6(6) (2010) 267–283.
[31] P. King, N. Rakesh, S. Beenalahari, Y. PrasannaKumar, V.S.R.K. Prasad, Removal of lead from aqueous solution using *Syzygium cumini* L.: Equilibrium and kinetic studies, J. Hazard. Mater. 142 (2007) 340–347.
[32] T. Santhi, S. Manonmani, Uptake of cationic dyes from aqueous solution by biosorption using granulized *Annona squmosa* Seed, E. J. Chem. 6(4) (2009) 1260–1266.
[33] A.E. Nemr, O. Abdelwahab, A. Khaled, A.E. Sikaily, Removal of chrysophenine dye (DY-12) from aqueous solution using dried *Ulva lactuca*, Egy. J. Aqua. Res. 31 (2005) 86–98.
[34] M. Rachakornkij, S. Ruangchuaya, S. Teachakulwiroj, Removal of reactive dyes from aqueous solution using bagasse fly ash, J. Sci. Technol. 26(1) (2004) 13–24.
[35] Y.X. Jiang, H.J. Xu, D.W. Liang, Z.F. Tong, Adsorption of basic violet 14 from aqueous solution on bentonite, Comptes Rendus Chimie 11 (2008) 125–129.
[36] D.H.K. Reddy, S.M. Lee, K. Seshaiah, Removal of Cd (II) and Cu(II) from aqueous solution by agro biomass: Equilibrium, kinetic and thermodynamic studies, Environ. Eng. Res. 17(3) (2012) 125–132.
[37] C.H.S. Gulipalli, B. Prasad, K.L. Wasewar, Batch study, equilibirum and kinetics of adsorption of sele-

nium using rice husk ash (RHA), J. Eng. Sci. Technol. 6 (2011) 586–605.
[38] G. Bayramoglu, B. Altintas, M.Y. Arica, Adsorption kinetics and thermodynamic parameters of cationic dyes from aqueous solutions by using a new strong cation-exchange resin, Chem. Eng. J. 152 (2009) 339–346.
[39] L. Li, S. Liu, T. Zhu, Application of activated carbon derived from scrap tires for adsorption of Rhodamine B, J. Environ. Sci. 22(8) (2010) 1273–1280.
[40] S. Patil, V. Deshmukh, S. Renukdas, N. Patel, Kinetics of adsorption of crystal violet from aqueous solutions using different natural materials, Int. J. Environ. Sci. 1 (6) (2011) 1116–1134.
[41] C.F. Chang, C.Y. Chang, K.H. Chen, W.T. Tsai, J.L. Shie, Y.H. Chen, Adsorption of naphthalene on zeolite from aqueous solution, J. Colloid Interface Sci. 277 (2004) 29–34.